STATISTICS, OPTIMIZATION AND INFORMATION COMPUTING
Stat., Optim. Inf. Comput., Vol. **14**, December 2025, pp 3874–3890.
Published online in International Academic Press (www.IAPress.org)

A Time-Delayed Mathematical Modeling for Monkeypox Transmission with Incubation Period

Muhammad Akbar Hidayat [1], Fatmawati [1,2,*], Cicik Alfiniyah [1], Olumuyiwa J. Peter [3,4,5]

[1]*Department of Mathematics, Faculty of Science and Technology, Universitas Airlangga, Surabaya 60115, Indonesia*
[2]*Department of Mathematics and Applied Mathematics, University of Johannesburg, Auckland Park, South Africa*
[3]*Department of Mathematics, Saveetha School of Engineering, SIMATS, Saveetha University, Chennai, Tamil Nadu, 602105, India*
[4]*Department of Mathematical and Computer Sciences, University of Medical Sciences, Ondo City, Ondo State, Nigeria*
[5]*Department of Epidemiology and Biostatistics, School of Public Health, University of Medical Sciences, Ondo City, Ondo State, Nigeria*

Abstract Monkeypox (mpox) is a re-emerging zoonotic disease whose global recurrence highlights the importance of quantitative understanding of its transmission patterns, notably the relevance of the incubation period. This study develops a time-delayed model that includes human, rodent, and environmental pathways. The incubation period is represented as a delay term. Analytical results show that the disease-free equilibrium remains stable for the fundamental reproduction number $R_0 < 1$, whereas an endemic equilibrium emerges when $R_0 > 1$. Sensitivity analyses show that R_0 is mostly influenced by human-to-human (β_1) and rodent-to-rodent (β_r) transmission rates. Numerical simulations are performed with varying time-delay values, representing different lengths of the incubation period. The results reveal that a longer incubation period leads to slower spread of the disease. In other words, the longer the incubation period, the more gradual the increase in the number of infected individuals over time. The suggested framework helps establish public health policies for outbreak forecasting, isolation timing, and environmental decontamination measures. It also serves as a decision-making tool for zoonotic disease control and preparedness.

Keywords Infectious Disease, Monkeypox, Delay Differential Equations, Parameter Estimation, Incubation Period

AMS 2010 subject classifications 92B05, 37N25, 34K99

DOI: 10.19139/soic-2310-5070-2875

1. Introduction

Monkeypox (mpox) is a zoonotic viral illness caused by the Monkeypox virus (MPXV), which belongs to the Orthopoxvirus genus in the Poxviridae family. Mpox, once endemic in Central and West Africa, has recently reemerged as a global health concern due to widespread outbreaks reported in more than 120 countries since 2022 [1, 2]. The virus is transmitted from animals to humans through direct contact with infected rodents or their bodily fluids, and from human to human through close physical contact, respiratory droplets, or contaminated objects [1]. Clinical manifestations include fever, headache, myalgia, lymphadenopathy, and a characteristic vesiculo-pustular rash that may present on various regions of the body. Severe cases can culminate in pneumonia, sepsis, or encephalopathy, particularly in immunocompromised individuals. As of late 2024, over 220 fatalities and more than 100,000 laboratory-confirmed cases have been recorded globally, underscoring the urgent necessity to understand the dynamics of mpox transmission and control strategies [2, 3, 4].

Mpox is transmitted through multiple interconnected routes that influence complex epidemiological dynamics. Human-to-human transmission is predominantly through direct contact with infectious skin lesions, bodily fluids,

*Correspondence to: F. Fatmawati (Email: fatmawati@fst.unair.ac.id). Department of Mathematics, Faculty of Science and Technology, Universitas Airlangga, Surabaya 60115, Indonesia.

ISSN 2310-5070 (online) ISSN 2311-004X (print)

or contaminated items such as clothing or bedding, as well as through the inhalation of droplets during extended face-to-face interactions. Recent outbreaks have shown that the virus is primarily concentrated in mucosal and lesion samples, supporting the predominant mode of transmission through close contact [4]. The zoonotic spillover from infected rodents or other wild mammals remains a considerable issue, since these species serve as reservoirs capable of transmitting the virus to humans by bites, wounds, or the handling of contaminated carcasses [5]. Research indicates that the monkeypox virus can persist on surfaces and textiles for several days to weeks, implying a potential risk of fomite transmission in certain circumstances, as environmental contamination contributes to secondary transmission [6].

The incubation period, which is the duration of time between the commencement of symptoms and the virus's exposure, typically corresponds to 6 to 13 days. Nevertheless, it could last up to 21 days, depending on the host's immunity, the virus load, and the mode of transmission [1]. The latent phase is crucial for understanding disease transmission, as asymptomatic or pre-symptomatic individuals might facilitate unnoticed spread, especially in densely populated or high-contact settings. Furthermore, data reveal variations in the incubation period across different epidemic circumstances; current analyses suggest that the duration of incubation is significantly affected by vaccination history and the mode of exposure [7, 8]. Therefore, it is crucial to accurately define this incubation period in order to create mathematical models that consider the duration between infection and infectiousness [9].

Mathematical modeling has emerged as a crucial tool for devising efficient public health interventions and understanding the transmission dynamics of mpox. Models are used to observe how the outbreak spreads and develops, estimate epidemiological parameters such as R_0, assess outbreak control thresholds, and simulate interventions or effects that influence the spread of the outbreak. Recent research has utilized fractional-order derivatives, time delays, and hybrid crossover dynamics to more effectively represent memory effects, latency periods, and intricate transmission channels [10]. While some have expanded classical compartmental frameworks to incorporate zoonotic spillover and environmental reservoirs, they recognize that the exclusion of these pathways can result in an underestimation of outbreak potential [11]. Modeling provides decision-makers with information regarding the most influential parameters (e.g., contact rates, rodent control, environmental decontamination) through sensitivity analysis and scenario simulation, thereby advising the prioritization of resources and the development of strategies. In order to predict future trends, assess combined human–animal–environment interventions, and ultimately manage the epidemic, it is imperative to implement resilient mathematical models in light of the present resurgence and global dissemination of mpox [12].

Numerous mpox models depict the incubation phase through an Exposed compartment, creating SEIR-type systems to illustrate the progression from infection to infectiousness [13]. Although this method accurately represents biological latency, numerous recent studies have demonstrated that the variability in immune response and incubation can be more accurately described by incorporating a time-delay term [10]. Delay-based formulations maintain biological realism without increasing model complexity by explicitly encoding infection memory in time, rather than through an additional compartment [14].

In the context of mpox transmission, recent research has drawn attention to the importance of environmental reservoirs, in which the virus can remain on surfaces or in aerosols for extended periods [6]. To account for this indirect route, a pathogen compartment (P) has been incorporated into numerous models, which represents the concentration of infectious agents in the environment [15]. This addition depicts interactions between human and rodent pathogens, which are frequently disregarded in frameworks that are solely based on the host. Recent studies have explored mpox transmission using diverse modeling frameworks to capture its zoonotic and environmental complexities. For instance, [16] developed a human–rodent interaction model to evaluate the role of reservoir hosts in amplifying outbreak risks in metropolitan areas. Similarly, [17] proposed a data-driven mpox model incorporating environmental pathogen persistence and optimal control measures, emphasizing the importance of including multiple transmission pathways in predicting outbreak dynamics. In addition, methodological insights from related infectious disease models, such as the SEIRS framework for tuberculosis that integrates environmental contamination and optimal control [18], provide valuable parallels for constructing realistic models of zoonotic diseases like mpox. These studies collectively demonstrate the relevance of incorporating both environmental and host dynamics, which motivates the formulation of our SIR–SI–P model to better represent the interconnected human, rodent, and environmental transmission routes of mpox. Motivated by these methods, our research creates

a SIR–SI–P model that combines environmental, rodent, and human dynamics to provide a more accurate depiction of mpox transmission.

Based on the evidence for human, rodent, and environmental transmission, this study suggests a SIR–SI–P compartmental model for mpox. To capture environmental contamination, the model has a pathogen compartment and human and rodent populations. The system is designed using a time-delay method to accurately model the incubation period in humans. The objectives of this work are to conduct sensitivity and stability analyses, as well as to analyze the dynamical behavior of the model. This framework delivers a comprehensive tool for comprehending mpox transmission and directing effective control strategies by integrating host and environmental dynamics.

2. Mathematical Model Formulation

2.1. Monkeypox Model Transmission

We consider a host-vector model for the transmission dynamics of monkeypox that incorporates an incubation period represented as a time delay τ. The host population (humans) is divided into three compartments: the susceptible humans S_h, the infected humans I_h, and the recovered humans R_h. The vector population (rodents) is classified into two compartments: the susceptible rodents S_r and the infected rodents I_r. In addition, we include an environmental compartment P that represents the concentration of pathogens (virus) present in the environment, which can contribute to the infection of humans.

The total human and rodent populations are given by

$$N_h = S_h + I_h + R_h, \qquad N_r = S_r + I_r.$$

Transmission of monkeypox in humans occurs through three main pathways: (i) direct human-to-human transmission with rate β_1, (ii) zoonotic transmission from rodents to humans with rate β_2, and (iii) exposure to pathogens in the environment with rate β_p. Rodent-to-rodent transmission is modeled with the parameter β_r.

Infected humans and rodents contribute to the concentration of environmental pathogens at rates θ_h and θ_r, respectively, while the environmental pathogen decays naturally at rate μ_p. To capture the incubation period, infection at a time t depends on the number of infectives at the past time $t - \tau$.

To establish the proposed model, the following assumptions are made regarding the transmission dynamics of monkeypox:

1. Susceptible humans (S_h) can be infected through contact with infected humans, infected rodents, or exposure to environmental pathogens (P), while susceptible rodents (S_r) can only be infected through contact with infected rodents.
2. The model incorporates a time delay (τ) to represent the incubation period, such that the number of new infections at time t depends on the number of infectious individuals at time $t - \tau$.
3. Infected humans and rodents contribute to the concentration of environmental pathogen at rates θ_h and θ_r, respectively, while pathogens decay naturally at rate μ_p.
4. Recruitment into the human and rodent populations occurs at constant rates Λ_h and Λ_r, respectively, with natural deaths at rates μ_h and μ_r. The concentration of pathogen in the environment decreases at rate μ_p.
5. Disease-induced deaths occur in both humans and rodents at rates δ_h and δ_r, respectively, while recovered humans (R_h) acquire permanent immunity.
6. The contact rates between humans, rodents, and the environment are heterogeneous and are influenced by ecological and behavioral factors.

The monkeypox transmission between human and rodent populations is fully provided in Figure 1.

The mathematical model of monkeypox spread with time delay by nonlinear autonomous system of ordinary differential equations is devoted as follows:

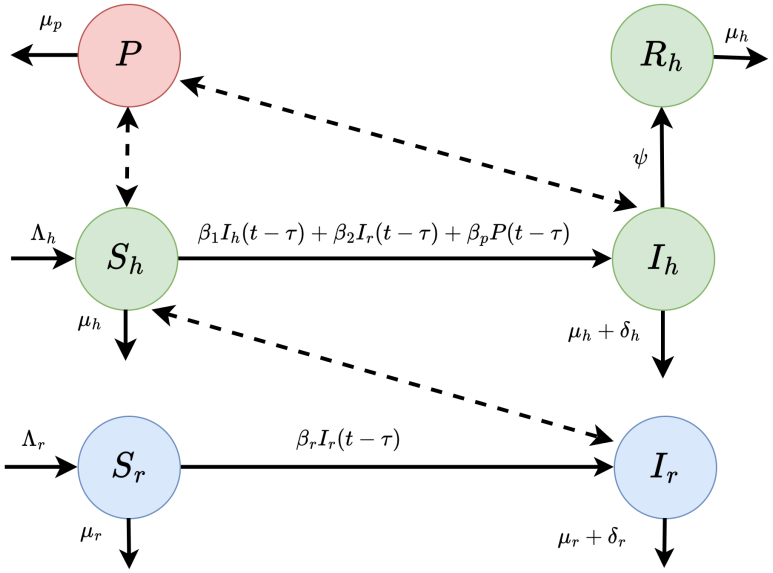

Figure 1. Diagram Transmission of Monkeypox with Patoghen

$$\begin{aligned}
\frac{dS_h}{dt} &= \Lambda_h - (\beta_1 I_h(t-\tau) + \beta_2 I_r(t-\tau) + \beta_p P)\, S_h - \mu_h S_h, \\
\frac{dI_h}{dt} &= (\beta_1 I_h(t-\tau) + \beta_2 I_r(t-\tau) + \beta_p P)\, S_h - (\psi + \mu_h + \delta_h) I_h, \\
\frac{dR_h}{dt} &= \psi I_h - \mu_h R_h, \\
\frac{dS_r}{dt} &= \Lambda_r - \beta_r I_r(t-\tau) S_r - \mu_r S_r, \\
\frac{dI_r}{dt} &= \beta_r I_r(t-\tau) S_r - (\mu_r + \delta_r) I_r, \\
\frac{dP}{dt} &= \xi_h I_h + \xi_r I_r - \mu_p P.
\end{aligned} \tag{1}$$

The notation and description of the parameters are given in Table 1.

2.2. *Positivity of the Solutions*

A population-based model is considered biologically consistent and meaningful only when all its state variables remain non-negative for every $t \geq t_0$. To ensure the epidemiological soundness of the SIR–SI–P model formulated in system (1), it is important to verify that all solutions of the system preserve their positivity over time. Specifically, the variables $S_h(t)$, $I_h(t)$, $R_h(t)$, $S_r(t)$, $I_r(t)$, and $P(t)$ must remain positive for all $t > t_0$.

Let $S_h(0)$, $I_h(0)$, $R_h(0)$, $S_r(0)$, $I_r(0)$, and $P(0)$ be the initial histories of system (1) on $[-\tau, 0]$. If all initial values are nonnegative, then the solution of system (1) satisfies

$$S_h(t),\ I_h(t),\ R_h(t),\ S_r(t),\ I_r(t),\ P(t) \geq 0 \quad \text{for all } t > 0.$$

Proof
We prove positivity by treating the four components separately.

Table 1. Description of model parameters

Parameter	Description
Λ_h	Recruitment rate of humans
Λ_r	Recruitment rate of rodents
β_1	Transmission rate from infected humans to susceptible humans
β_2	Transmission rate from infected rodents to susceptible humans
β_r	Transmission rate from infected rodents to susceptible rodents
β_p	Transmission rate from environmental pathogens to susceptible humans
μ_h	Natural death rate of humans
μ_r	Natural death rate of rodents
μ_p	Natural decay rate of pathogens in the environment
δ_h	Disease-induced death rate of humans
δ_r	Disease-induced death rate of rodents
ψ	Recovery rate of infected humans
ξ_h	Contribution rate of infected humans to environmental pathogens
ξ_r	Contribution rate of infected rodents to environmental pathogens
τ	Time delay (incubation period)

1. Human susceptible ($S_h(t)$).
From system (1) we have

$$\frac{dS_h(t)}{dt} = \Lambda_h - \big(\beta_1 I_h(t-\tau) + \beta_2 I_r(t-\tau) + \beta_p P(t-\tau)\big) S_h(t) - \mu_h S_h(t).$$

Set

$$\eta_h(t) = \beta_1 I_h(t-\tau) + \beta_2 I_r(t-\tau) + \beta_p P(t-\tau) \geq 0.$$

Then

$$\frac{dS_h(t)}{dt} \geq -(\eta_h(t) + \mu_h) S_h(t).$$

Multiplying by the integrating factor $e^{\mu_h t + \int_0^t \eta_h(s)\, ds}$ and integrating from 0 to t gives

$$S_h(t) \geq S_h(0) \exp\Big(- \mu_h t - \int_0^t \eta_h(s)\, ds \Big) > 0,$$

so $S_h(t) \geq 0$ for all $t \geq 0$.

The same calculation applies to $S_r(t)$ by setting $\eta_r(t) = \beta_r I_r(t-\tau) \geq 0$, hence $S_r(t) \geq 0$ for all $t \geq 0$.

2. Human infected ($I_h(t)$).
Assume, to the contrary, that there exists $t_1 > 0$ minimal such that $I_h(t_1) = 0$ while $I_h(t) \geq 0$ for $t \in [-\tau, t_1]$. From the infected-human equation of system (1):

$$\frac{dI_h(t)}{dt} = \big(\beta_1 I_h(t-\tau) + \beta_2 I_r(t-\tau) + \beta_p P(t-\tau)\big) S_h(t) - (\psi + \mu_h + \delta_h) I_h(t).$$

At $t = t_1$, by minimality we have $I_h(t_1 - \tau) \geq 0$, $I_r(t_1 - \tau) \geq 0$, $P(t_1 - \tau) \geq 0$, and $S_h(t_1) \geq 0$. Thus

$$\frac{dI_h(t_1)}{dt} = \big(\beta_1 I_h(t_1-\tau) + \beta_2 I_r(t_1-\tau) + \beta_p P(t_1-\tau)\big) S_h(t_1) \geq 0,$$

which contradicts the minimality of t_1. Therefore $I_h(t) \geq 0$ for all $t \geq 0$.

The same contradiction argument applies to $I_r(t)$ (use the rodent infected equation), hence $I_r(t) \geq 0$ for all $t \geq 0$.

3. Human recovered ($R_h(t)$).
From the recovered equation:

$$\frac{dR_h(t)}{dt} = \psi I_h(t) - \mu_h R_h(t).$$

Since $I_h(t) \geq 0$, we have

$$\frac{dR_h(t)}{dt} \geq -\mu_h R_h(t).$$

Multiplying by $e^{\mu_h t}$ and integrating from 0 to t yields

$$\frac{d}{dt}\left(e^{\mu_h t} R_h(t)\right) \geq 0 \quad \Longrightarrow \quad R_h(t) \geq R_h(0) e^{-\mu_h t} \geq 0,$$

thus $R_h(t) \geq 0$ for all $t \geq 0$.

4. Environmental pathogen ($P(t)$).
Let the pathogen contributions be denoted by $\xi_h, \xi_r \geq 0$ so that

$$\frac{dP(t)}{dt} = \xi_h I_h(t) + \xi_r I_r(t) - \mu_p P(t).$$

Since $I_h(t), I_r(t) \geq 0$, it follows that

$$\frac{dP(t)}{dt} \geq -\mu_p P(t).$$

Multiplying by $e^{\mu_p t}$ and integrating from 0 to t gives

$$\frac{d}{dt}\left(e^{\mu_p t} P(t)\right) \geq 0 \quad \Longrightarrow \quad P(t) \geq P(0) e^{-\mu_p t} \geq 0,$$

thus $P(t) \geq 0$ for all $t \geq 0$.

Thus all state variables of system (1) remain nonnegative for every $t > 0$. This completes the proof of Theorem 2.2. □

2.3. Invariant Region

The invariant region represents the domain in which all solutions of the proposed SIR–SI–P model described in system (1) are biologically and mathematically relevant. All parameters in the model are assumed to be non-negative for all $t \geq t_0$. Furthermore, solutions that begin with positive initial conditions remain non-negative for all $t \geq t_0$ and are bounded within a biologically feasible region.

The set of state variables $S_h(t)$, $I_h(t)$, $R_h(t)$, $S_v(t)$, $I_v(t)$, and $P(t)$ of the SIR–SI–P model given in (1) is confined within a positive and bounded feasible region denoted by Ω.

Proof
Define $N_h(t) = S_h + I_h + R_h$ and $N_r(t) = S_r + I_r$. Summing the human equations gives

$$\frac{dN_h}{dt} = \Lambda_h - \mu_h S_h - (\psi + \mu_h + \delta_h) I_h - \mu_h R_h = \Lambda_h - \mu_h N_h - \delta_h I_h \leq \Lambda_h - \mu_h N_h.$$

By comparison with $\dot{X} = \Lambda_h - \mu_h X$, it follows that

$$N_h(t) \leq \max\left\{N_h(0), \frac{\Lambda_h}{\mu_h}\right\} \quad \text{for all } t \geq 0,$$

and in particular $N_h(t) \leq \Lambda_h/\mu_h$ for large t.

Similarly, summing the rodent equations yields

$$\frac{dN_r}{dt} = \Lambda_r - \mu_r S_r - (\mu_r + \delta_r)I_r = \Lambda_r - \mu_r N_r - \delta_r I_r \leq \Lambda_r - \mu_r N_r,$$

hence

$$N_r(t) \leq \max\left\{N_r(0), \frac{\Lambda_r}{\mu_r}\right\} \quad \text{for all } t \geq 0.$$

From the pathogen equation

$$\frac{dP}{dt} = \xi_h I_h + \xi_r I_r - \mu_p P \leq \xi_h N_h^{\max} + \xi_r N_r^{\max} - \mu_p P,$$

where $N_h^{\max} = \Lambda_h/\mu_h$ and $N_r^{\max} = \Lambda_r/\mu_r$. Comparison with the linear equation $\dot{Z} = \xi_h N_h^{\max} + \xi_r N_r^{\max} - \mu_p Z$ yields

$$P(t) \leq \max\left\{P(0), \frac{\xi_h N_h^{\max} + \xi_r N_r^{\max}}{\mu_p}\right\} \quad \text{for all } t \geq 0.$$

Combining positivity with the above upper bounds shows that any trajectory starting in $\mathbb{R}^6_+$ remains in Ω for all $t \geq 0$, so Ω is positively invariant. This completes the proof. □

3. Discussion

3.1. Equilibrium Analysis

In this section, we determine the equilibrium points of the monkeypox model (1) under the presence of a constant delay (τ). Specifically, we determine the steady states by assuming that the delayed terms satisfy $I_h(t) = I_h(t-\tau)$ and $I_r(t) = I_r(t-\tau)$ at equilibrium. The model (1) admits two possible equilibria: disease-free equilibrium (DFE) and endemic equilibrium (EE). The detailed derivations for each case are presented in the following subsections.

3.1.1. Disease-Free Euilibrium (DFE) The disease-free equilibrium is provided by:

$$E_0 = (S_h^0, I_h^0, R_h^0, S_r^0, I_r^0, P^0) = \left(\frac{\Lambda_h}{\mu_h}, 0, 0, \frac{\Lambda_r}{\mu_r}, 0, 0\right).$$

3.1.2. Basic Reproduction Number (R_0) Then, we compute the basic reproduction number (R_0) that can be utilized to quantify the possibility of the transmission for the infection in the population. By using the Next Generation Matrix method [19], the matrices F (new infection part) and Z (transition part) assessed at the disease-free equilibrium (E_0) are presented respectively as follows:

$$F = \begin{pmatrix} \beta_1 S_h^0 & \beta_2 S_h^0 & \beta_p S_h^0 \\ 0 & \beta_r S_r^0 & 0 \\ 0 & 0 & 0 \end{pmatrix}, \qquad V = \begin{pmatrix} \psi + \mu_h + \delta_h & 0 & 0 \\ 0 & \mu_r + \delta_r & 0 \\ -\xi_h & -\xi_r & \mu_p \end{pmatrix}.$$

The basic reproduction number (R_0) is determined by the spectral radius ρ (dominant eigenvalue in magnitude) of the matrix FZ^{-1}. Therefore, R_0 for model (1) can be written as:

$$R_0 = \max\{R_{0h}, R_{0r}\} = \max\left\{\frac{\Lambda_h(\xi_h\beta_p + \mu_p\beta_1}{\mu_h\mu_p(\psi + \mu_h + \delta_h)}, \frac{\beta_r}{(\mu_r + \delta_r)}\right\}.$$

3.1.3. Existence of Endemic Equilibria Furthermore, from the results of the analytical calculations, we suppose $\kappa = (\beta_1 I_h^* + \beta_2 I_r + \beta_p P)$ the endemic equilibrium point of the system (1) is obtained as follows:

$$E^* = (S_h^*, I_h^*, R_h^*, S_r^*, I_r^*, P^*)$$

with

$$\begin{aligned}
S_h^* &= \frac{\Lambda}{(\kappa + \mu_h)},\\
I_h^* &= \frac{\kappa S_h^*}{m_1},\\
R_h^* &= \frac{\psi I_h^*}{\mu_h},\\
S_r^* &= \frac{\mu_r}{\beta_r},\\
I_r^* &= \frac{\mu_r}{\beta_r}(R_{0r} - 1),\\
P^* &= \frac{\xi_h \left(\frac{\kappa S_h^*}{m_1}\right) + \xi_r \left(\frac{\mu_r}{\beta_r}(R_{0r} - 1)\right)}{\mu_p},
\end{aligned}$$

and consider the value of κ, it yields:

$$a\kappa^2 + b\kappa + c = 0$$

where

$$\begin{aligned}
a &= m_1 \beta_r,\\
b &= m_1 \mu_h \beta_r - (\beta_1 \beta_r \Lambda_h + m_1 \beta_2 \mu_r (R_{0r} - 1) + \beta_r \beta_p \xi_h \Lambda_h + m_1 \beta_p \xi_r \mu_r (R_{0r} - 1)),\\
c &= -m_1 \mu_h \beta_2 \mu_r (R_{0r} - 1) - m_1 \mu_h \beta_p \xi_r \mu_r (R_{0r} - 1).
\end{aligned}$$

Here, the coefficient a is always positive, while the positivity of the coefficient c depends on the sign of R_{0r}. If $R_{0r} < 1$ then $c > 0$, while for $R_{0r} > 1$, we have $c < 0$.

Further discussion on these can be shown in the following statements:

1. If $c < 0$ or $R_{0r} > 1$, then there exists a unique endemic equilibrium, since one root is positive and the other negative ($\kappa_1 \kappa_2 < 0$).
2. If $b < 0$ and either $c = 0$ or $b^2 - 4ac = 0$, then there exists a unique endemic equilibrium corresponding to a degenerate case.
3. If $c > 0$, $b < 0$ and $b^2 - 4ac > 0$, then there exists the possibility of two endemic equilibria.
4. Otherwise, there is no endemic equilibrium.

3.2. Stability Analysis

Based on system (1), we linearize the mathematical modeling with time delay as

$$\det\left(\lambda I - J_0 - J_1 e^{-\lambda \tau_1}\right) = 0 \tag{2}$$

where

$$J_0 = \begin{pmatrix}
-(\beta_1 I_h(t-\tau) + \beta_2 I_r(t-\tau) + \beta_p P(t-\tau)) - \mu_h & 0 & 0 & 0 & 0 & 0\\
(\beta_1 I_h(t-\tau) + \beta_2 I_r(t-\tau) + \beta_p P(t-\tau)) & -(\mu_h + \delta_h) & 0 & 0 & 0 & 0\\
0 & \psi & -\mu_h & 0 & 0 & 0\\
0 & 0 & 0 & \beta_r I_r(t-\tau) - \mu_r & 0 & 0\\
0 & 0 & 0 & \beta_r I_r(t-\tau) & -(\mu_r + \delta_r) & 0\\
0 & 0 & \xi_h & 0 & \xi_r & -\mu_p
\end{pmatrix}$$

and

$$J_1 = \begin{pmatrix} 0 & -\beta_1 S_h & -\beta_2 S_h & -\beta_p S_h & 0 & 0 \\ 0 & \beta_1 S_h & \beta_2 S_h & \beta_p S_h & 0 & 0 \\ 0 & 0 & 0 & 0 & 0 & 0 \\ 0 & 0 & 0 & -\beta_r S_r & 0 & 0 \\ 0 & 0 & 0 & \beta_r S_r & 0 & 0 \\ 0 & 0 & 0 & 0 & 0 & 0 \end{pmatrix}.$$

3.2.1. Stability of DFE The local stability of the disease-free equilibrium point is obtained by substituting the value of the disease-free equilibrium point $E_0 = \left(S_h^0, I_h^0, R_h^0, S_r^0, I_r^0, P^0\right) = \left(\frac{\Lambda_h}{\mu_h}, 0, 0, \frac{\Lambda_r}{\mu_r}, 0, 0\right)$ into the (2), so we obtain the eigenvalues:

$$\lambda_1 = -\mu_h, \quad \lambda_2 = -\mu_h \quad \lambda_3 = -\mu_r$$

and the other eigenvalues are given as follows:

$$\lambda + (\mu_r + \delta_r) - \frac{\Lambda_r}{\mu_r} e^{-\lambda\tau} = 0, \tag{3}$$

$$(\lambda^2 + \lambda\left((\psi + \mu_h + \mu_p + \delta_h) - \frac{\beta_1 \Lambda_h}{\mu_h} e^{-\lambda\tau}\right)) + \mu_p(\psi + \mu_h + \delta_h) - \left(\frac{\xi_h \beta_p \Lambda_h}{\mu_h} + \frac{\mu_p \beta_1 \Lambda_h}{\mu_h}\right) e^{-\lambda\tau} = 0. \tag{4}$$

Condition without delay Suppose $\tau = 0$, the equation (3) reduces to $\lambda = \frac{\Lambda_r}{\mu_r} - (\mu_r + \delta_r) = \frac{1}{(\mu_r + \delta_r)}(\frac{\frac{\Lambda_r}{\mu_r}}{(\mu_r + \delta_r)} - 1) = \frac{1}{(\mu_r + \delta_r)}(R_{0r} - 1)$. Thus, DFE is locally asymptotically stable if $R_{0r} < 1$.

Condition with delay Suppose $\tau > 0$, the term $e^{-\lambda\tau}$ of the equation (3) may induce oscillatory dynamics. To determine whether delay can destabilise the system, we look for purely imaginary roots $\lambda = i\omega$.
Substituting $\lambda = i\omega$ into (3), it yields the following

$$\begin{cases} (\mu_r + \delta_r) - \frac{\Lambda_r}{\mu_r} \cos(\omega\tau) = 0, \\ \omega + \frac{\Lambda_r}{\mu_r} \sin(\omega\tau) = 0. \end{cases}$$

Using some algebraic manipulation, we obtain

$$(\mu_r + \delta_r)\sqrt{(R_0 + 1)(R_0 - 1)}.$$

It is clear that there is no solution for $\omega > 0$ for $R_{0r} < 1$. Therefore, the roots of (3) must be real. Furthermore, for real λ, define $f(\lambda) := \lambda + (\mu_r + \delta_r) - \frac{\Lambda_r}{\mu_r} e^{-\lambda\tau}$. It can be seen that $f'(\lambda) = 1 + \frac{\Lambda_r}{\mu_r}\tau e^{-\lambda\tau} > 0$, so f is strictly increasing on $\mathbb{R}$. Consider the limits $\lim_{\lambda\to-\infty} f(\lambda) = -\infty$ and $\lim_{\lambda\to\infty} f(\lambda) = \infty$. Hence, there is exactly one root. If $\frac{\Lambda_r}{\mu_r} < (\mu_r + \delta_r)$ then $f(0) = (\mu_r + \delta_r) - \frac{\Lambda_r}{\mu_r} < 0$ so the unique real root is negative.

Let the equation (4) be $\lambda^2 + (p + qe^{-\lambda\tau})\lambda + r + se^{-\lambda\tau} = 0$
where

$$\begin{aligned} p &= (\psi + \mu_h + \mu_p + \delta_h), \\ q &= -\frac{\beta_1 \Lambda_h}{\mu_h}, \\ r &= \mu_p(\psi + \mu_h + \delta_h), \\ s &= -\left(\frac{\xi_h \beta_p \Lambda_h}{\mu_h} + \frac{\mu_p \beta_1 \Lambda_h}{\mu_h} e^{-\lambda\tau}\right). \end{aligned}$$

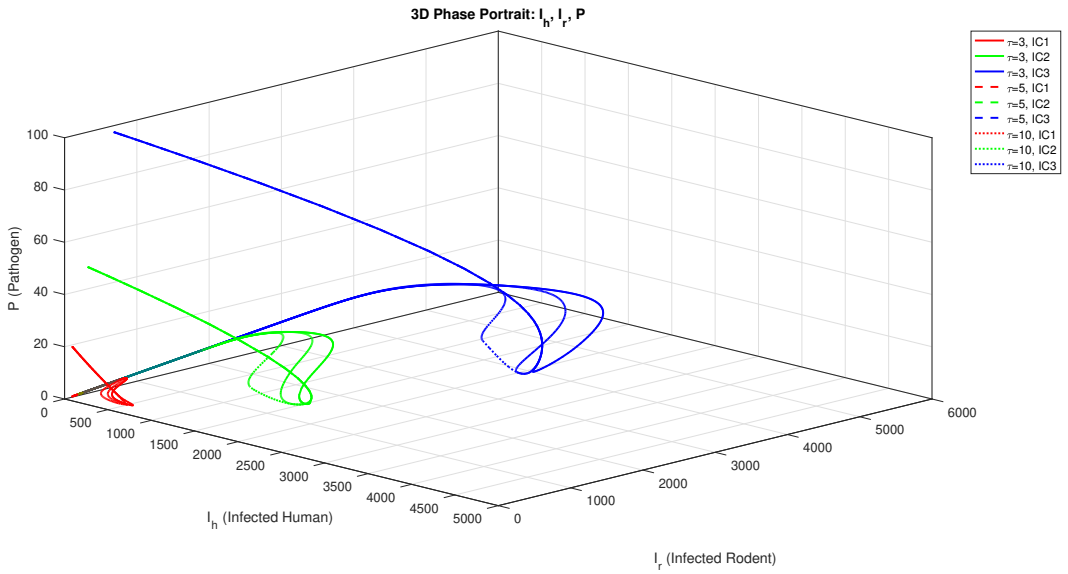

Figure 2. Phase Portrait

Condition without delay Suppose $\tau = 0$, the equation reduces to $\lambda^2 + p\lambda + (r + s) = 0$. The equilibrium is asymptotically stable if only if both coefficients of the quadratic are positive. Consider $p > 0 \Leftrightarrow (\psi + \mu_h + \mu_p + \delta_h) - \frac{\beta_1 \Lambda_h}{\mu_h} > 0 \Leftrightarrow 1 > R_{0h}$. Thus, stability of DFE is asymptotically stable.

Condition with delay When $\tau > 0$, without losing of generality. We subtitute $\lambda = i\omega$ into equation (4). It yields the following:

$$\begin{cases} -\omega^2 + r - s\cos(\omega\tau) - q\omega\sin(\omega\tau) = 0, \\ p\omega - q\omega\cos(\omega\tau) + s\sin(\omega\tau) = 0 \end{cases}$$

Using some algebraic manipulation, it follows that: $\omega^4 + (-2r + p^2 - q^2)\omega^2 + (r^2 - s^2) = 0$
Suppose $u := \omega^2 >= 0$, it yields:
$u^2 + mu + n = 0$
where

$$m = -2r + p^2 - q^2, \qquad n = r^2 - s^2$$

To ensure that equation (4) has negative real roots, we apply the Routh–Hurwitz criterion. According to this criterion, the conditions $m > 0$ and $n > 0$ must be satisfied.
Starting with the condition $n > 0$, we have $r^2 - s^2 > 0$, leading to $b^2(1 + R_{0h})(1 - R_{0h}) > 0$. It follows that $n > 0$ is satisfied whenever $R_{0h} < 1$. Moving on to the second condition, $m > 0$ corresponds to $-2r + p^2 - q^2 > 0$ will lead us to $(p + q)(p - q) > 2r$.

3.2.2. Stability of EE The stability of the endemic equilibrium (EE) is analytically complex to determine. Therefore, we analyze its behavior using a phase portrait based on the initial conditions employed in the numerical simulation, as presented in Table 2. The corresponding phase portrait is illustrated in Figure 2.

The trajectories in Figure 2 show that variations in the delay parameter τ produce distinct oscillatory behaviors. For smaller delays ($\tau = 3$), the system tends to converge toward equilibrium faster, whereas larger delays ($\tau = 10$) induce prolonged oscillations before stabilizing, reflecting the impact of infection latency on disease persistence.

3.3. Sensitivity Analysis

The sensitivity analysis quantifies the relative impact of each parameter on the basic reproduction numbers R_{0h} and R_{0r}. Parameters with the largest absolute values of the sensitivity index indicate the most influential factors affecting the variation of R_0.

The sensitivity index of R_0 with respect to a given parameter m is defined as [20, 21]:

$$\Upsilon_m^{R_0} = \frac{\partial R_0}{\partial m} \times \frac{m}{R_0}.$$

This index measures the relative change in R_0 resulting from a relative change in the parameter m. A positive sensitivity index indicates that an increase in m leads to an increase in R_0, whereas a negative value implies the opposite effect. Using the parameter values listed in Table 2, the computed sensitivity indices for R_{0h} and R_{0r} are summarized in Table 3.

From the results, it can be observed that the parameters β_1, δ_h, β_r, and δ_r have the greatest influence on R_0. Specifically, β_1 and β_r positively influence R_0, implying that an increase in the transmission rate among humans or rodents will enhance the spread of infection. Conversely, δ_h and δ_r exhibit negative sensitivity indices, indicating that an increase in recovery or removal rates will reduce R_0.

To further explore the effects of these key parameters, we conducted numerical simulations by varying the values of β_1 and β_r. This allows us to assess how changes in these transmission rates directly affect infection dynamics, including the peak infection level and the total number of infected individuals over time. Such analysis provides insight into which control strategies—such as reducing contact rates or enhancing recovery—would be most effective in mitigating disease spread.

Table 2. Parameter values used in the monkeypox model.

Parameter	Value	Unit	Source
Λ_h	0.3	individual $\times$ day^{-1}	[22]
μ_h	0.001	day^{-1}	[22]
β_1	0.001	(individual $\times$ day)$^{-1}$	[22, 23]
β_2	0.005	(individual $\times$ day)$^{-1}$	[24, 25]
β_p	0.001	(pathogen unit $\times$ day)$^{-1}$	[24, 26]
ψ	0.09	day^{-1}	[27, 23]
δ_h	0.01	day^{-1}	[22, 28]
Λ_r	0.6	individual $\times$ day^{-1}	[24, 22]
μ_r	0.004	day^{-1}	[27, 23]
β_r	0.0002	(individual $\times$ day)$^{-1}$	[24, 25]
δ_r	0.003	day^{-1}	[24, 28]
ξ_h	0.001	pathogen unit $\times$ (individual $\times$ day)$^{-1}$	[29, 23]
ξ_r	0.0015	pathogen unit $\times$ (individual $\times$ day)$^{-1}$	[24, 26]
μ_p	0.5	day^{-1}	[29]

Table 3. Parameter Sensitivity Index

Parameters	**Sensitivity Index** (R_{0h})	**Sensitivity Index** (R_{0r})
β_1	0.998	–
β_p	0.0019	–
μ_h	-1.0099	–
μ_p	-0.0019	–
δ_h	-0.09	–
ψ	-0.891	–
ξ_h	0.0019	–
β_r	–	1
μ_r	–	-1.57
δ_r	–	-0.43

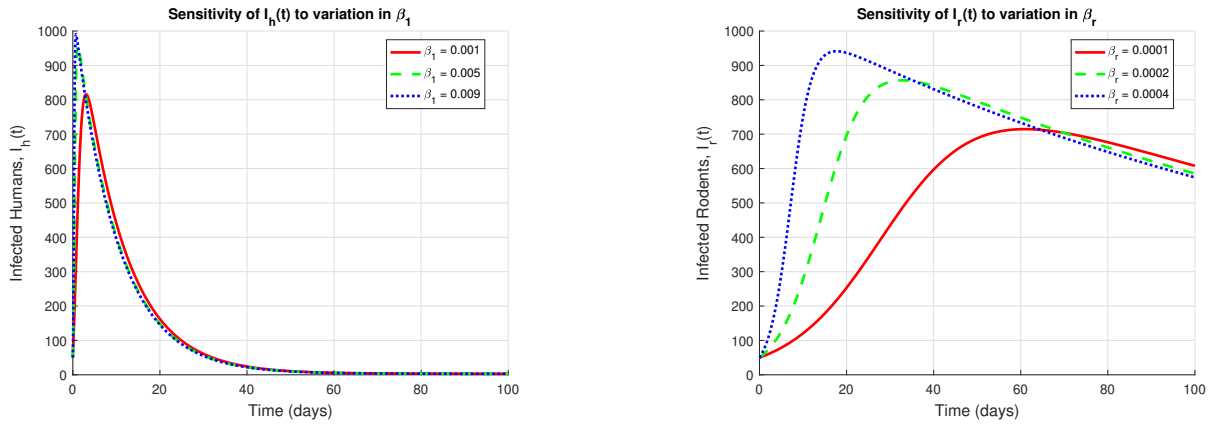

(a) Impact of β_1 on the Infected Human Population

(b) Impact of β_r on the Infected Rodent Population

Figure 3. Impact of particular parameters for each population

Looking at Figure 3a, it is apparent that although β_1 directly influences the infected human population, its variation also indirectly affects the infected human population. As the value of β_1 increases, the rate of transmission between humans increases, resulting in a higher number of infections and a more sustained outbreak. Conversely, reducing β_1 through interventions such as improved hygiene, public health measures, or vaccination can lead to significant decreases in R_0, thus mitigating the scale of the epidemic. This result supports the work of [22]. In public health terms, the high sensitivity of R_0 to β_1 indicates that interventions such as contact tracing, isolation of symptomatic cases, and targeted vaccination of high-risk groups would be particularly effective in reducing disease transmission. Similarly, the effect of β_r on the infected rodent population can be seen in Figure 3b. Reducing β_r through environmental sanitation or vector control measures could therefore limit rodent-to-human transmission and decrease the overall infection pressure on the human population.

3.4. Numerical Simulation

In this section, the dynamic behavior of the time-delay model (1) is examined through numerical integration using the parameter values listed in Table 2 and Table 4. Two parameter sets are considered to represent distinct epidemiological regimes: the *disease-free case* ($R_0 < 1$) and the *endemic case* ($R_0 > 1$). The delay parameter τ is varied to investigate its influence on the temporal evolution of the system, reflecting the biological effect of incubation or transmission delay.

Table 4. Parameter values used in the monkeypox transmission model under disease-free equilibrium condition.

Parameter	Value	Source
Λ_h	0.03913894	[22]
μ_h	3.9139×10^{-5}	[22]
β_1	1.0×10^{-6}	[22, 23]
β_2	5.0×10^{-7}	[24, 25]
β_p	5.0×10^{-7}	[24, 26]
ψ	0.15	[27, 23]
δ_h	0.001	[22, 28]
Λ_r	5.0	[24, 22]
μ_r	0.01	[27, 23]
β_r	1.0×10^{-5}	[24, 25]
δ_r	0.001	[24, 28]
ξ_h	0.001	[29, 23]
ξ_r	0.05	[24, 26]
μ_p	0.2	[29]

For the disease-free condition, simulations are performed with relatively low transmission rates ($\beta_1 = 1.0 \times 10^{-6}$, $\beta_2 = 5.0 \times 10^{-7}$, and $\beta_r = 1.0 \times 10^{-5}$). The results, illustrated in Figure 4, show that all trajectories converge to the disease-free equilibrium E_0, confirming its local stability.

In both human and rodent populations, the infected compartments (I_h and I_r) and the pathogen concentration (P) decline to zero as time progresses. Increasing the delay τ slightly postpones the infection peak but does not change the overall outcome, indicating that the infection eventually dies out in all cases. The observed transient oscillations gradually disappear, demonstrating that the system remains stable despite the inclusion of delay.

To represent the endemic condition, the transmission parameters are increased to $\beta_1 = 0.001$, $\beta_2 = 0.005$, and $\beta_r = 0.0002$, while keeping other biological parameters as shown in Table 2. The simulation results in Figure 5 indicate that all state variables approach nonzero steady states, confirming convergence to the endemic equilibrium E_1.

In this case, both human and rodent infections initially rise, reaching a peak before settling at stable endemic levels. As the delay τ increases, the peak values of I_h, I_r, and P become smaller and occur later in time, suggesting that a longer incubation or transmission delay slows the spread of infection but does not eliminate it. The model therefore captures the gradual adjustment toward endemic equilibrium, with reduced oscillations as time progresses.

The numerical results in Figures 4–5 demonstrate that varying the delay parameter τ affects only the transient dynamics of the system, particularly the timing and amplitude of infection peaks. However, the qualitative long-term behavior—convergence to the disease-free equilibrium when $R_0 < 1$ and to the endemic equilibrium when $R_0 > 1$—remains unchanged. These findings confirm the analytical stability results and highlight the moderating role of time delay in the transmission process.

Subsequent study may rectify these limitations by integrating regional heterogeneity, temporal variability, and uncertainty analysis. These extensions would augment the model's use in evaluating the dynamics of monkeypox and facilitate more context-specific public health decision-making.

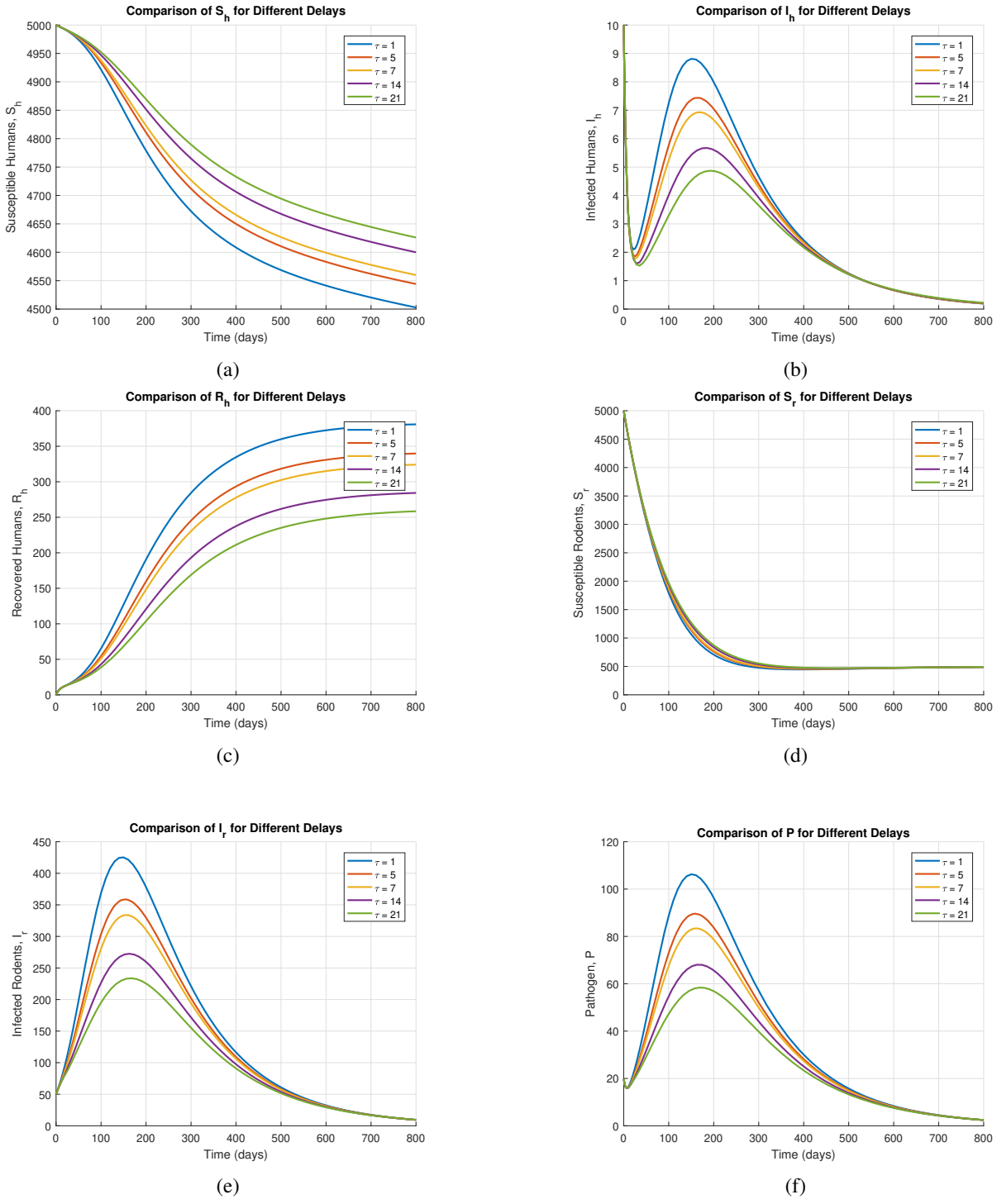

Figure 4. Disease-Free Situation Numerical Simulation; (a-c) Human Population, (d-e) Rodent Population, (f) Pathogen

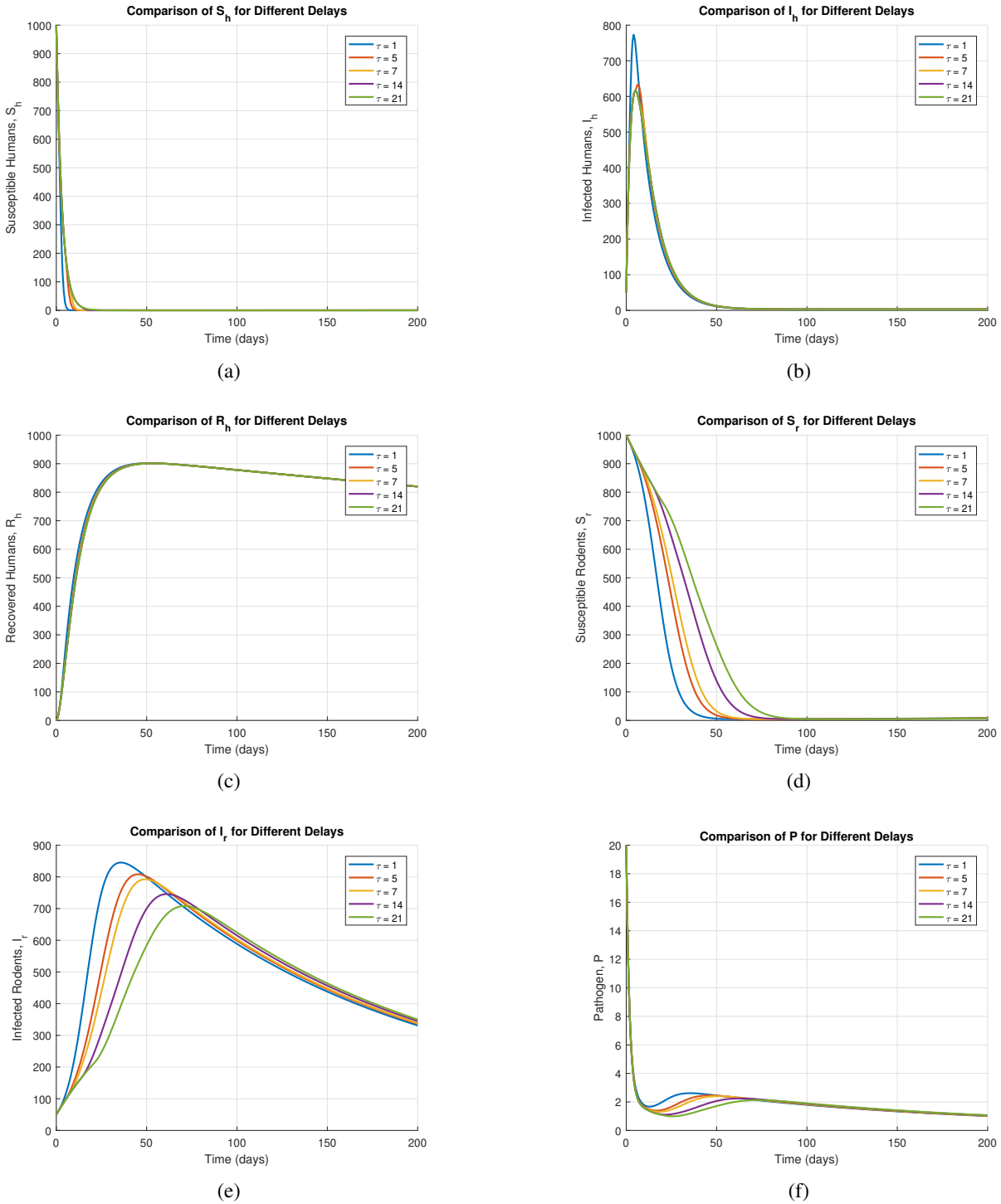

Figure 5. Endemic Situation Numerical Simulation; (a-c) Human Population, (d-e) Rodent Population, (f) Pathogen

3.5. Public Health Implication and Control Strategies

The results of this study reveal that the incubation period plays a critical role in shaping the temporal dynamics of monkeypox transmission. A longer delay between infection and symptom onset can suppress the early growth

of infections but prolong the epidemic's overall duration. This finding highlights the importance of implementing timely interventions during the incubation phase. Strengthening contact tracing, improving active surveillance, and enforcing early quarantine of exposed individuals can substantially reduce secondary infections. Additionally, combining these measures with vaccination and vector control efforts during the pre-symptomatic stage could enhance the overall effectiveness of outbreak containment.

4. Recommendation

In light of the model's findings, it is recommended that national surveillance systems incorporate the time-delay effect between exposure and detectability. Developing early warning systems that explicitly account for this incubation delay can help public health authorities anticipate future infection surges more accurately. Efforts should focus on proactive detection, contact monitoring, and the rapid isolation of exposed individuals before the onset of symptoms.

Furthermore, the integration of model-based insights into epidemic preparedness frameworks will improve the timeliness and precision of interventions. Enhancing diagnostic capacity, promoting public awareness about asymptomatic transmission, and encouraging self-reporting behavior among at-risk populations can significantly improve outbreak management. Future modeling studies should consider incorporating demographic heterogeneity and environmental influences to strengthen predictive capability and policy relevance.

5. Conclusion

This study formulated a delay differential model to elucidate the transmission dynamics of monkeypox, integrating the incubation period (represented as a time delay) and the environmental pathogen population as an alternative infection pathway. The incorporation of this environmental component allows the model to account for indirect transmission via contaminated environments, so offering a more accurate depiction of disease dissemination.

Analytical findings demonstrate that the disease-free equilibrium (E_0) is locally asymptotically stable for $R_0 < 1$, but numerical simulations utilizing phase portraits suggest that the endemic equilibrium (E_1) is locally asymptotically stable for $R_0 > 1$. The temporal delay τ affects transient dynamics without altering long-term stability, highlighting its essential role in illness persistence.

However, this study has several limitations. The model assumes homogeneous mixing within and between human and rodent populations, whereas contact patterns may vary across geographic, social, and ecological contexts. Parameter values were obtained from existing literature and may not fully represent local epidemiological conditions. Additionally, all parameters were treated as constant over time, despite the fact that behavioral changes, interventions, and environmental factors can modify transmission dynamics.

Notwithstanding these constraints, the results underscore the significance of integrating both environmental transmission and incubation delay into monkeypox models, providing critical insights for formulating control strategies centered on early detection, isolation, and sanitation of the environment.

Authorship contribution statement

Muhammad A. Hidayat: conceptualization, methodology, software, formal analysis, visualization, writing—original draft preparation. **F. Fatmawati:** conceptualization, validation, investigation, resources, writing—review and editing, supervision. **Cicik Alfiniyah:** writing—review and editing, supervision. **Olumuyiwa J. Peter:** validation, writing—review and editing.

REFERENCES

1. World Health Organization (WHO). (2024). *Mpox – Fact Sheet.* Updated August 2024. Available from: https://www.who.int/news-room/fact-sheets/detail/mpox.
2. Centers for Disease Control and Prevention (CDC). (2024). *Mpox in the United States and Around the World: Current Situation.* Updated September 2024. Available from: https://www.cdc.gov/mpox/situation-summary/.
3. World Health Organization (WHO). (2024). *Multi-Country Outbreak of Mpox: External Situation Report #44 – 23 December 2024.* Available from: https://www.who.int/publications/m/item/multi-country-outbreak-of-mpox--external-situation-report-44---23-december-2024.
4. Thornhill, J. P., et al. (2022). Monkeypox Virus Infection in Humans across 16 Countries. *New England Journal of Medicine*, **387**(8), 679–691. doi:10.1056/NEJMoa2207323.
5. Adepoju, O. A., et al. (2024). An Optimal Control Model for Monkeypox Transmission Involving Human and Rodent Populations. *PLOS ONE*, **19**(2), e0300451.
6. Morgan, C. N., Whitehill, F., Doty, J. B., et al. (2022). Environmental Persistence of Monkeypox Virus on Surfaces in Household of a Person with Travel-Associated Infection, Dallas, Texas, USA, 2021. *Emerging Infectious Diseases*, **28**(7), 1455–1459. doi:10.3201/eid2807.220401.
7. World Health Organization (WHO). (2025). *Mpox: Key Facts and Epidemiological Overview.* Updated February 2025. Available from: https://www.who.int/news-room/fact-sheets/detail/mpox.
8. Miura, F., et al. (2022). Estimating the Incubation Period of Monkeypox Virus during the 2022 Multi-Country Outbreak. *Euro Surveillance*, **27**(37):2200448. doi:10.2807/1560-7917.ES.2022.27.37.2200448.
9. Guarner, J., et al. (2023). Monkeypox 2022: What Clinicians Need to Know. *Lancet Infectious Diseases*, **23**(5), e120–e128. doi:10.1016/S1473-3099(22)00878-2.
10. Sweilam, N. H., Al-Mekhlafi, S. M., Hassan, S. M., Alsenaideh, N. R., & Radwan, A. E. (2024). A Novel Hybrid Crossover Dynamics of Monkeypox Disease Mathematical Model with Time Delay: Numerical Treatments. *Fractal and Fractional*, **8**(4), 185. doi:10.3390/fractalfract8040185.
11. Liu, G., & Li, H. (2024). Dynamical Analysis of a Class of Monkeypox Epidemic Model. *Thermal Science*, **28**(4B), 3367–3383. doi:10.2298/TSCI2404367L.
12. Frank, T. D. (2024). Mathematical Analysis of Four Fundamental Epidemiological Models for Monkeypox Disease Outbreaks: On the Pivotal Role of Human–Animal Order Parameters. *Mathematics*, **12**(20), 3215. doi:10.3390/math12203215.
13. Buonomo, B., Della Marca, R., & d'Onofrio, A. (2024). Modeling the Spread of Monkeypox: Stability and Bifurcation Analysis of an SEIR-Type Model. *Chaos, Solitons & Fractals*, **181**, 114673.
14. Qi, Y., Zhang, Y., & He, X. (2023). Analysis of a Time-Delay SEIR Model for Monkeypox Transmission Dynamics. *Mathematical Biosciences and Engineering*, **20**(12), 23451–23472.
15. Okyere, E., et al. (2024). Mathematical Modeling of Monkeypox Virus Transmission Considering Environmental Contamination. *PLOS ONE*, **19**(3), e0302451.
16. Yuan, L., Li, R., Zhang, J., & Chen, X. (2022). Assessing transmission risks and control strategy for monkeypox as an emerging zoonosis in a metropolitan area. *Journal of Medical Virology*, **95**(1), e28137. https://doi.org/10.1002/jmv.28137
17. Ochieng, V. B., Okoth, J. A., & Otieno, G. (2025). Mathematical modeling of Mpox virus dynamics with a case study of Africa. *Modeling Earth Systems and Environment*. https://doi.org/10.1007/s40808-025-02369-0
18. Ochieng, V. B., Okoth, J. A., & Otieno, G. (2025). SEIRS model for TB transmission dynamics incorporating the environment and optimal control. *BMC Infectious Diseases*, **25**, 10710. https://doi.org/10.1186/s12879-025-10710-2
19. van den Driessche, P., & Watmough, J. (2002). Reproduction numbers and sub-threshold endemic equilibria for compartmental models of disease transmission. *Mathematical Biosciences*, **180**, 29–48.
20. Marino, S., Hogue, I. B., Ray, C. J., & Kirschner, D. E. (2008). A methodology for performing global uncertainty and sensitivity analysis in systems biology. *Journal of Theoretical Biology*, **254**(1), 178–196.
21. Chitnis, N., Hyman, J. M., & Cushing, J. M. (2008). Determining important parameters in the spread of malaria through the sensitivity analysis of a mathematical model. *Bulletin of Mathematical Biology*, **70**(5), 1272–1296.
22. Peter, O. J., Kumar, S., Kumari, N., & others. (2022). Transmission dynamics of Monkeypox virus: a mathematical modelling approach. *Modeling Earth Systems and Environment*, **8**, 3423–3434. https://doi.org/10.1007/s40808-021-01313-2
23. Helikumi, M., et al. (2025). Dynamical Analysis of Mpox Disease with Environmental (fractional-order model). *Mathematics*, **9**(6), 356. https://www.mdpi.com/2504-3110/9/6/356.
24. Madubueze, C. E., Onwubuya, I. O., Nkem, G. N., & Chazuka, Z. (2022). The transmission dynamics of the monkeypox virus in the presence of environmental transmission. *Frontiers in Applied Mathematics and Statistics*, **8**, 1061546. https://www.frontiersin.org/articles/10.3389/fams.2022.1061546/full.
25. Onifade, A. A., et al. (2025). Modeling monkeypox transmission with a compartmental approach. *Scientific Reports*, **15**, 10852. https://www.nature.com/articles/s41598-025-10852-y.
26. Das, H. K., et al. (2024). Exploring the dynamics of monkeypox transmission with environmental and human-to-human interactions. *Frontiers in Public Health*, **12**, 11150605. https://pmc.ncbi.nlm.nih.gov/articles/PMC11150605/.
27. Peter, O. J., Kumar, S., Kumari, N., Oguntolu, F. A., Oshinubi, K., & Musa, R. (2021). Mathematical modeling of monkeypox virus transmission dynamics. *Journal of Infection in Developing Countries*, **15**(12), 1908–1917.
28. Qian, M., et al. (2025). An epidemiological model of monkeypox. *BMC Infectious Diseases*, **25**, 10873. https://bmcinfectdis.biomedcentral.com/articles/10.1186/s12879-025-10873-y.
29. Yinda, C. K., Morris, D. H., Fischer, R. J., et al. (2023). Stability of Monkeypox Virus in Body Fluids and Wastewater. *Emerging Infectious Diseases*, **29**(10). https://wwwnc.cdc.gov/eid/article/29/10/23-0824_article.